Temporal Evolution of Beam Emittance
from a Field Emission Electron Gun

G. Bekefi, F. Hartemann and D.A. Kirkpatrick

Temporal Evolution of Beam Emittance from a Field Emission Electron Gun

G. Bekefi, F. Hartemann and D.A. Kirkpatrick

Department of Physics and Research Laboratory of Electronics,

Massachusetts Institute of Technology

Cambridge, Massachusetts, 02139

Abstract

The temporal evolution of the beam emittance and beam brightness from a field emission electron gun (1.3 MV, 0.5 kA, 30 ns) has been measured with nanosecond time resolution, using a novel Čerenkov-electrooptic diagnostic. Observations show that guns provided with velvet-backed cathodes behave differently, and are superior to, the more conventional graphite cathodes.

1. Introduction

Intense relativistic electron beams find application in many diverse areas including x-ray production[1], laser pumping[2], material response studies[3], generation of coherent electromagnetic radiation[4], and inertial confinement fusion[5]. The generation of such beams entails use of electron guns equipped with field emission (explosive emission) cathodes which are capable of providing current densities ranging from hundreds to thousands of amperes per square centimeter of surface area.

In many applications[4,5] high beam quality as exemplified by a low beam emittance ϵ_n, and a high beam brightness B_n, is of paramount importance. In this paper, we report what we believe is the first detailed study of the temporal evolution of these quantities. Measurements, obtained using a novel Čerenkov-electrooptic shutter, show that guns provided with velvet-backed[6] cathodes behave differently, and are superior to the more conventional graphite cathodes. In addition, such time resolved measurements may help towards our understanding of the complex cathode phenomena studied by many workers during the past two decades, and ably summarized by Hinshelwood[7].

2. Experimental arrangement

The overall experimental setup is shown in Fig.1. A Physics International Pulserad 110A electron accelerator is used to energize a five stage multielectrode field emission gun[8]. The resulting paraxial electron beam (1.3 MV,0.5 kA,30 ns), of radius $r_b \simeq 2.5$ cm, impinges on a 1 mm thick tantalum disc. A small pinhole aperture 0.5 mm in diameter allows a low current (~ 0.2 A) beamlet to propagate in a 35 cm field free region before it strikes a 3 mm thick Plexiglas plate used as a Čerenkov radiator. The Čerenkov radiation is then sampled by an electrooptic crystal gated for a few hundred picoseconds and recorded on regular 35 mm film after amplification by a pulsed microchannel image intensifier[9].

The emittance is determined by observing the photographed spot sizes, which is directly proportional to the beamlet microscopic spread angle $\delta\theta$ (see Fig.1), at a given time in the voltage pulse. Different photographs, taken at different times, then allow one to observe the temporal evolution of the beam emittance. A variable delay allows the sampling of the Čerenkov light at different times in the voltage pulse. The relative timing

of the optical gate in the electron beam pulse is recorded on each shot by a dual beam oscilloscope. The temporal accuracy of these measurements is approximately 1 ns. Neutral density light attenuators placed in front of the electrooptic shutter are used to supply a known linear intensity scale for the optical system and to insure that the film emulsion operates in the "gray zone". The optical gate used for the experiments described here is 1.8 ns wide. The insert to Fig.1 illustrates the photographed spot sizes at four consecutive times during the voltage pulse, for the graphite and velvet cathodes, respectively. We note that whereas the spot sizes for the velvet cathode remain virtually unchanged with time, those for graphite decrease substantially as time increases. The evolution of voltage and beam current as a function of time, spanning the full range of emittance measurements, is illustrated in Fig.2.

The unnormalized beam emmitance ϵ is given by $\epsilon \simeq r_b(v_\perp/v_\parallel) \simeq r_b\delta\theta$, where $v_\perp$ and $v_\parallel$ are the transverse and axial electron velocities, respectively ; and r_b is the effective beam radius. Both $\delta\theta$ and r_b are functions of time t during the voltage pulse, although the variations of r_b are relatively small (for velvet r_b lies in the range 2.6-2.8 cm, for graphite in the range 2.1-2.5 cm). Thus ϵ can be obtained directly from a knowledge of the electron beam radius r_b and the measured beamlet spread angle $\delta\theta$. More accurately[8], we first measure the film density of the photographed images with a photodensitometer. The beamlet image is moved (in what we will call the x-direction) across a slit which is larger than the extent of the image in the y-direction, and narrow in the x-direction. In this way, we effectively integrate over all velocities in one transverse dimension, while determining the velocity distribution in the other transverse dimension. This velocity distribution is then appropriately weighted by the current density profile of the beam $J(r,t)$, measured independently using a series of concentric circular collectors connected to a low inductance calibrated current viewing resistor, and a phase space contour is then plotted as a function of the transverse coordinate x, and $\theta_x = v_x/v_z$. Finally, the emittance[3] ϵ is defined as $1/\pi$ times the area in the $x-\theta_x$ plane of the projection of the phase space volume that encloses 90% of the electrons. The normalized emittance is then given by $\epsilon_n = \beta\gamma\epsilon$ where $\beta = v/c$ is the normalized beam velocity, and $\gamma = 1 + (eV/m_0c^2)$ is the relativistic mass factor (V is the accelerator voltage). Once the emittance and beam current I are determined, the normalized beam brightness can be

calculated from $B_n = I/\pi^2 \epsilon_n^2$.

3. Results

Figure 3 illustrates the temporal behavior of the beamlet microscopic spread angle $\delta\theta$ as a function of time for a reactor graphite cathode and a velvet-backed cathode. Except for the change of emitting materials, the experimental conditions for graphite and velvet are the same. The cathode plate consists of a large (5 cm radius) spin-formed aluminum disk with a cylindrical hole in the middle which allows the insertion of a 1 cm radius plug of emitting material. The remainder of the cathode surface is covered with a hard aluminum oxide (anodized) coating to minimize undesired emission[8] . An electric field $E = 210$ kV/cm is applied between the cathode and the first (extraction) anode (anode-cathode gap $d = 1.55$ cm). Four additional electrodes then accelerate the beam to its final energy. At the gun exit, the electron beam radius equals ~ 2.5 cm. Henceforth we shall discuss the quantity $\gamma\beta\delta\theta$ rather than $\delta\theta$ itself. The reason is that, barring emittance growth and large changes of r_b within the gun and transport line, $\gamma\beta\delta\theta$ is an invariant ; this is consistent with the notion that the normalized emittance is conserved during the acceleration process.

A number of different mechanisms can contribute to $\gamma\beta\delta\theta$. These include lensing at the extraction anode ; finite thermal velocities of the electrons emitted from the cathode ; patchy emission in which the overall beam evolves from microscopic plasma emission sites which are in the process of merging to form a surface plasma which ultimately becomes the source of the electron beam ; surface roughness of the ensuing plasma ; and beamlet expansion due to self-electrostatic forces. The total emittance can be estimated by simply summing over these different contributions (a more exact way of summing the various contributions would require an accurate knowledge of the electron velocity distribution function).

In our experiments, lensing[10] is readily accounted for. It comes about as a result of the fact that the extraction and final anodes consist of transmitting tungsten meshes. This results in an irreducible $[\gamma\beta\delta\theta]_{mesh} \simeq 6$ mrad. The remainder of the observed $\gamma\beta\delta\theta$ is attributed to cathode related processes.

4

Figures 2 and 3 show that graphite and velvet behave in markedly different ways. In the case of the velvet-backed cathode it is readily calculated from the current-voltage characteristics of Fig.2 that space-charge limited (Child-Langmuir) flow is attained rapidly, in less than $\sim$ 5 ns, at which time $\gamma\beta\delta\theta \simeq 20$ mrad. Substracting $[\gamma\beta\delta\theta]_{mesh}$, leaves $\gamma\beta\delta\theta$ of $\sim$ 14 mrad believed to be caused at the cathode.

Thermal effects are found to be too small to explain the observed emittance, and patchy emission (unlike that for graphite discussed below) has not been observed in the case of velvet [11]. We speculate that surface roughness of the plasma-coated cathode may well be an important contributor. Surface roughness, recently studied theoretically by Lau [12] primarily in regard to thermionic cathodes, causes field lines to diverge from the protusions, thereby giving electrons a component of velocity parallel to the cathode plane. Applying Lau's calculations to field emission cathodes shows that for protusions of height h (and width $\lesssim h$)

$$\gamma\beta\delta\theta \simeq 0.1(Jh^2)^{1/3} \quad \text{(rad)}, \tag{1}$$

where J is the space-charge limited current density in the anode-cathode gap. Taking $h = 30\,\mu$m which is typical [7] of surface roughness, and using the measured current density $J = 3 \times 10^6$ A/m^2, yields $\gamma\beta\delta\theta \simeq 14$ mrad, in agreement with observations. It is also noteworthy that on the basis of equation (1), the beam brightness scales with current density as $B_n \sim J^{1/3}$ which is in rough conformity with earlier time-integrated brightness measurements [13].

The picture is quite different in the case of the graphite cathode. We see from Fig.2 that the turn-on time is quite long, and the current takes some 20 ns to reach its maximum value. The observed length of turn-on time is in good agreement with earlier observations [14] which show that this time is a strong function of the applied electric field and cathode material. Calculations made from the voltage-current characteristics of Fig.2 also indicate that space-charge limited flow is not attained at any time during the voltage pulse. From Fig.3 we see that unlike the case of velvet, $\delta\theta$ is now a strong function of time and $\gamma\beta\delta\theta$ varies between $\sim$ 33 mrad at early times and $\sim$ 16 mrad at late times. Substracting the contribution to $\gamma\beta\delta\theta$ associated with lensing (see above), leaves a range of $\gamma\beta\delta\theta$ from $\sim$ 27 mrad at early times to $\sim$ 10 mrad at late times attributable to cathode related

effects.

The poor performance of graphite is believed to be the result of patchy, incomplete [7,15] turn-on of the cathode at the relatively low applied electric field of 210 kV/cm. This conforms with earlier time-integrated measurements [8,13] which show that electric fields in excess of ~ 400 kV/cm are needed for complete turn-on of graphite cathodes. Several experiments have shown that the overall beam evolves from microscopic emission sites [16,17] located on the cathode. Electrons stream from these sites in the form of secondary conical beamlets [15] whose number density N has been estimated [7] to be $\sim 10^2 - 10^4$ cm^{-2}.

A portion of the net $\gamma\beta\delta\theta$ that needs to be accounted for (10–27 mrad) in graphite is believed to be due to space-charge repulsion within the individual beamlets. Calculating the transverse motion of an electron in the combined radial self-electric field and the azimuthal self-magnetic field, one finds that

$$\gamma\beta\delta\theta \simeq \alpha\sqrt{I_b/I_A} \quad \text{(rad)}. \tag{2}$$

Here $I_b = J/N$ is the beamlet current and $I_A = (4\pi\epsilon_0 m_0 c^3/e)\gamma\beta = 17\gamma\beta$ (kA) is the Alfvén current ; $\alpha \simeq 2\sqrt{\log(a/a_0)}$ is a dimensionless constant with a and a_0 as the initial and final beamlet radii. Over the cathode-anode gap distance, the beamlet radii increases by $\sim 20\,\%$, with the result that $\alpha \simeq 1$. Taking $I_b \simeq 1$ A yields $\gamma\beta\delta\theta \simeq 4$ mrad. Surface roughness may well account for the remaining spread in $\delta\theta$.

The observed decrease of $\gamma\beta\delta\theta$ with time by a factor of ~ 3 is not fully understood. One may conjecture [7] interactions between beamlets. However, calculations show that purely quasi-electrostatic forces between beamlets have no effect on the spread angle $\delta\theta$. An alternate form of interaction [18] comes about as a result of the fact that the space-charge field of an existing beamlet shields the neighboring cathode surface from the applied field. This reduces the likelihood of further beamlet formation via the explosive field-emission process. Details as to how this may affect $\delta\theta$ are not clear.

4. Conclusion

In conclusion, our time-resolved studies of the beam emittance from field-emission (explosive emission) cathodes illustrate the importance of proper choice of cathode material.

The lower emittance associated with velvet-backed cathodes compared with the more conventional graphite cathodes leads to higher beam brightness, as is clearly illustrated in Fig.4. Why velvet cathodes, unlike graphite cathodes, exhibit complete and rapid turn-on at electric fields as low or lower than ~ 200 kV/cm is not understood at present. However, there is circumstantial evidence that gaseous and/or solid impurities occluded in the fabric fibers play an important role. Rapid, repetitive pulsing of the electron gun, which presumably removes occluded impurities, lowers [19] the electron beam brightness.

Acknowledgements

References

[1] R. Gillette, Science **188**, 30 (1975)

[2] L.P. Bradley, Inst. Phys. Conf. Series **29**, 58 (1976)

[3] R.B. Oswald, F.B. McLean, D.R. Shallhorn and L.D. Buxton, J. Appl. Phys. **42**, 3463 (1971)

[4] C.W. Roberson, Proc. Soc. Photo-Opt. Int. Eng. **453**, 320 (1983)

[5] L.I. Rudakov, Proc. Conf. Plasma Physics and Cont. Nuclear Fusion Research (Baltimore 1982), Nuclear Fusion Supplement 1983 p. 393

[6] R.J. Adler, G.F. Kiuttu, B.E. Simpkins, D.J. Sullivan and D.E Voss, Mission Research Corp. Albuquerque, New Mexico, Report No AMRC-N-275 (1984)

[7] D.D. Hinshelwood, Naval Research Laboratory Memorandum Report No 5492 (1985)

[8] D.A. Kirkpatrick, R.E. Shefer and G. Bekefi, J. Appl. Phys. **57**, 5011 (1985)

[9] F. Hartemann and G. Bekefi, Appl. Phys. Lett. **49**, 1680 (1986)

[10] G.R. Brewer in *"Focussing of Charged Particles"*, ed. A. Septier (Academic Press, New York 1967) p. 35

[11] R.E. Klinkowstein and R.E. Shefer, Bull. APS **31**, 1396 (1986) and private communication

[12] Y.Y. Lau, Naval Research Laboratory Memorandum Report No 5853 (1986)

[13] G. Bekefi, R.E. Shefer and S.C. Tasker, Nuc. Inst. and Methods in Phys. Res. **A250**, 91 (1986)

[14] R.K. Parker, R.E. Anderson and C.V. Duncan, J. Appl. Phys. **45**, 2463 (1974). Also S.P. Bugaev, G.A. Mesyats and D.I. Proskurovskii, Sov. Phys., Doklady **14**, 605 (1969)

[15] O. Milton, IEEE Trans. Elec. Insul. **El-9**, 68 (1974)

[16] G.A. Lyubimov and V.I. Rakhovskii, Sov. Phys. Usp. **21**, 693 (1978)

[17] R.L. Boxmann, S.L. Goldsmith, I. Israeli and S. Shalev, IEEE Trans. Plasma Science **11**, 138 (1983)

[18] S. Ya'Belomyttsev, S.D. Korovin and G.A. Mesyats, Sov. Tech. Phys. Letters **6**, 466 (1980)

[19] T.J. Orzechowski (private communication)

Figure captions

Fig.1 Experimental arrangement and (insert) photographs of beamlet sizes at three different times during the voltage pulse for velvet and graphite cathodes.

Fig.2 Beam voltage and current as a function of time during the voltage pulse, for velvet and graphite cathodes.

Fig.3 Averaged beamlet spread angle $\delta\theta$ (see Fig.1) as a function of time for velvet and graphite cathodes, defined as $\delta\theta(t) = \epsilon(t)/r_b(t)$.

Fig.4 Normalized beam brightness B_n as a function of time for velvet and graphite cathodes.

GATED ELECTROOPTIC SHUTTER

CAMERA

MIRROR

ZnS SCINTILATOR

GATED MICROCHANNEL IMAGE INTENSIFIER

ČERENKOV PLATE

$2\delta\theta$

APERTURE DISK

ELECTRON BEAM

MARX ACCEL- ERATOR
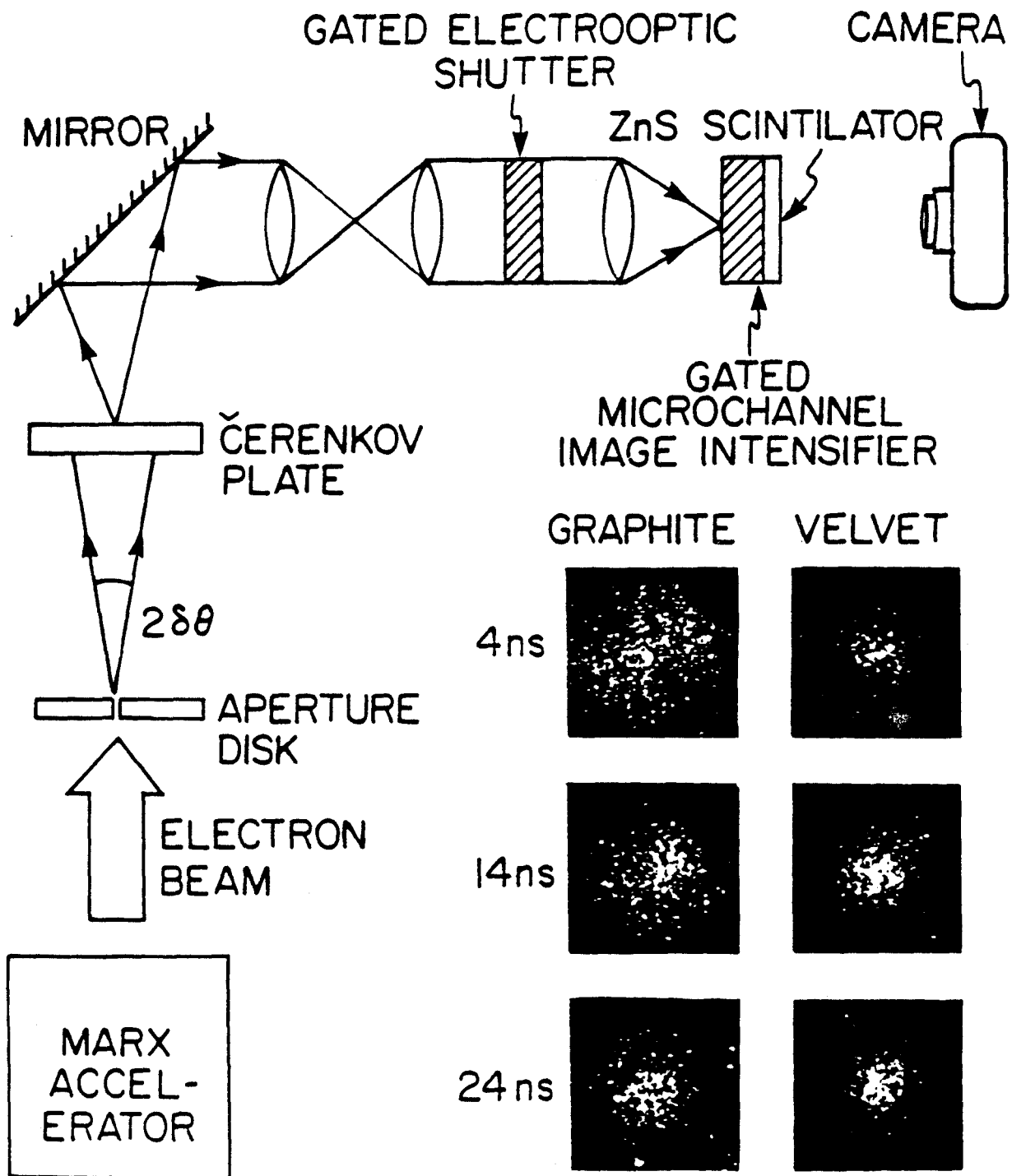
GRAPHITE VELVET

4ns

14ns

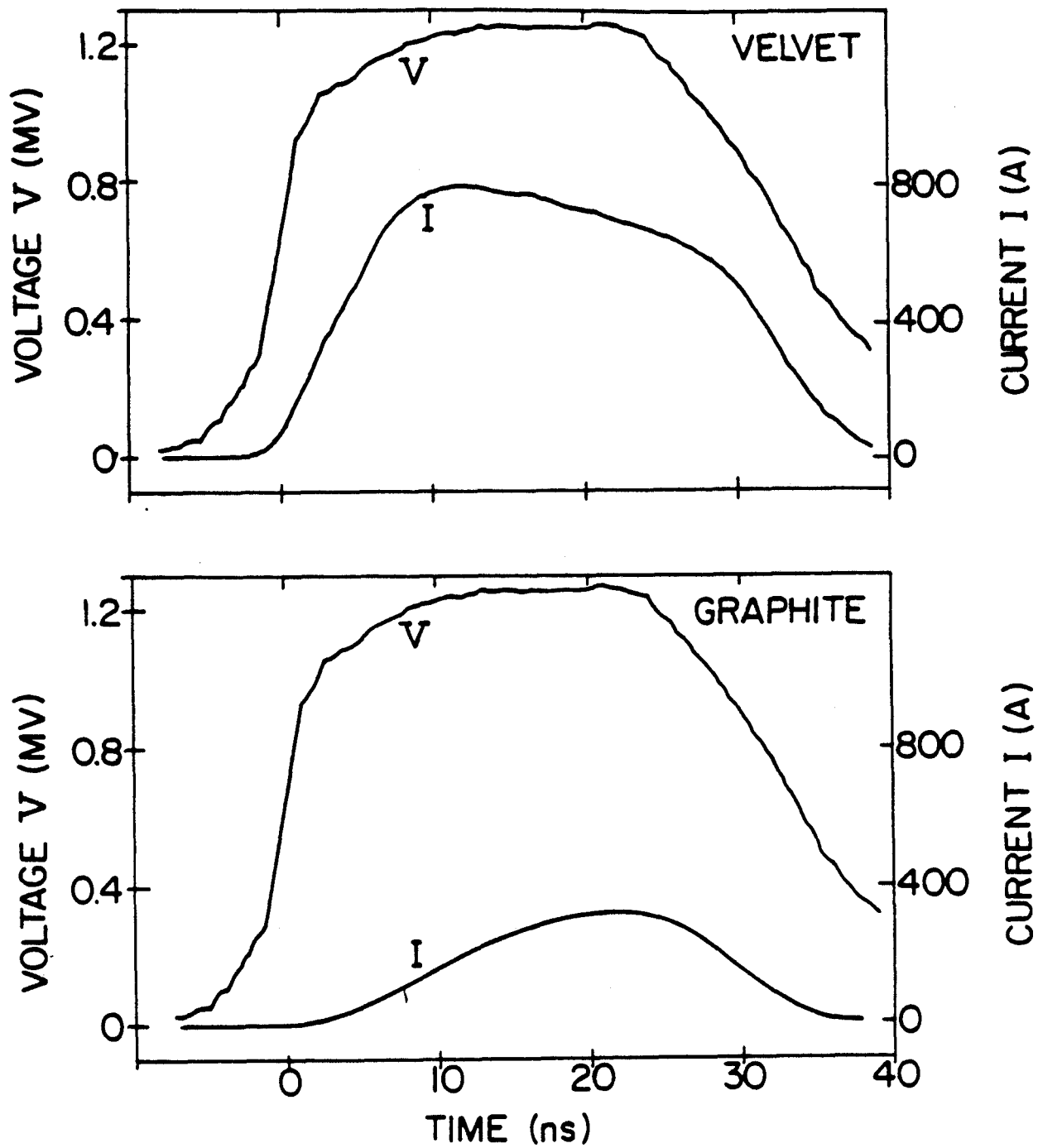24 ns

Fig. 1
Bekefi, Hartemann, Kirkpatrick
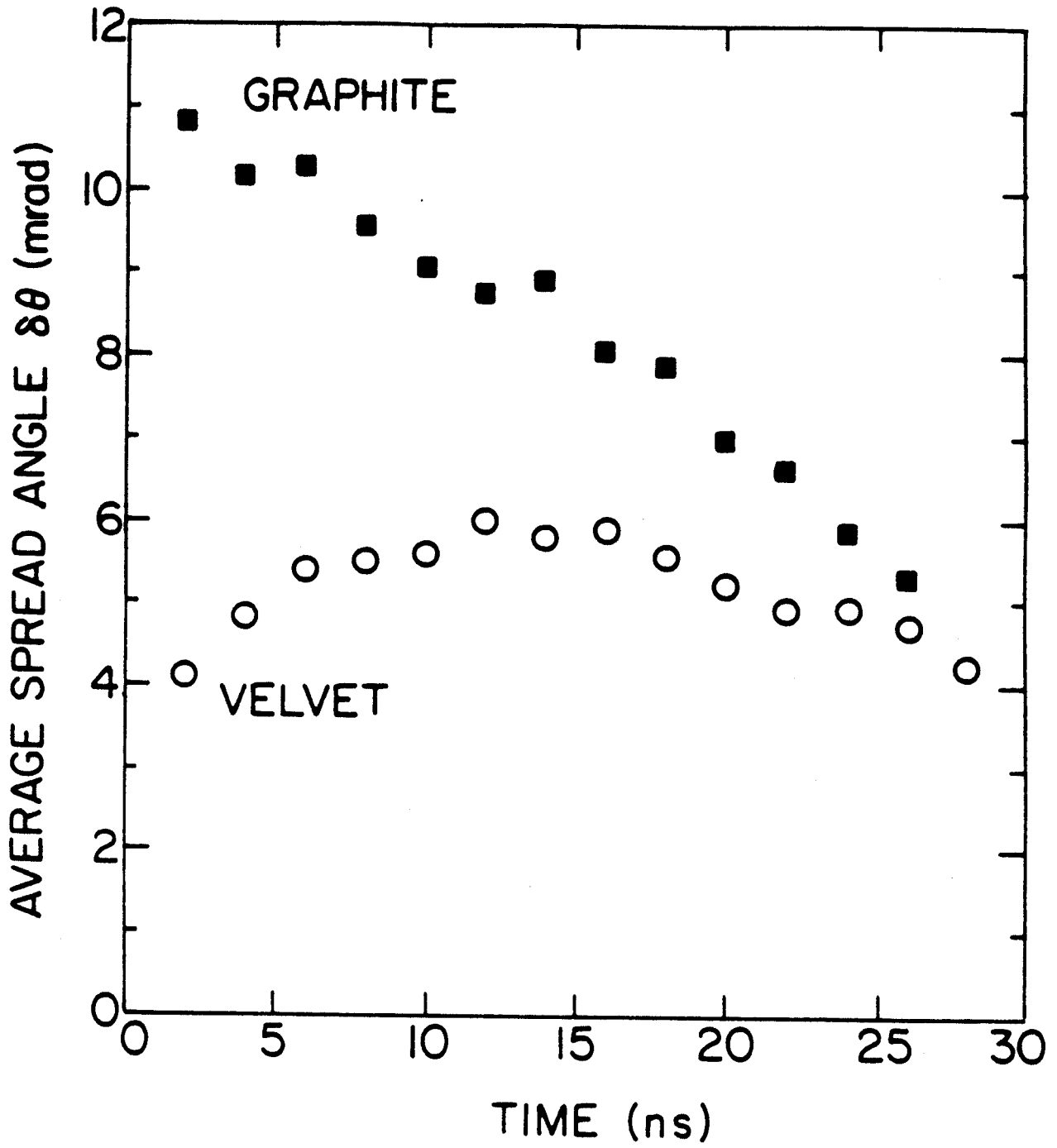
Fig. 2
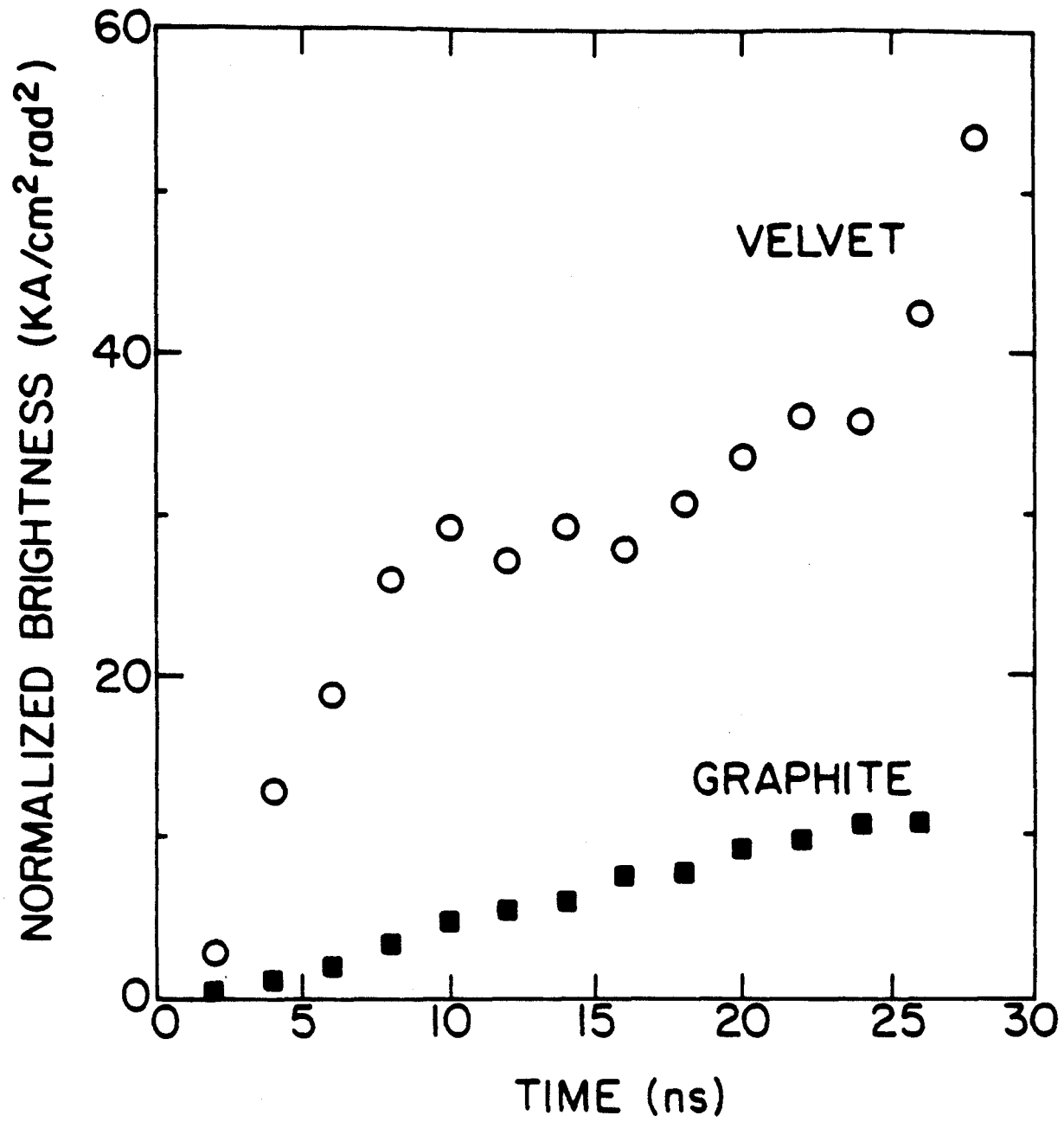Bekefi, Hartemann, Kirkpatrick

Fig. 3
Bekefi, Hartemann, Kirkpatrick

Fig. 4
Bekefi, Hartemann, Kirkpatrick